Electroanatomic Mapping of Arrhythmogenic Right Ventricular Dysplasia

Munther Boulos, MD, Ilan Lashevsky, MD, Shimon Reisner, MD, Lior Gepstein, MD, PhD
Haifa, Israel

OBJECTIVES   We tested the hypothesis that spatial association of low-amplitude intracardiac electrograms can identify the presence, location and extent of dysplastic regions in arrhythmogenic right ventricular dysplasia (ARVD).

BACKGROUND   Arrhythmogenic right ventricular dysplasia is a right ventricular (RV) cardiomyopathy characterized pathologically by fibrofatty infiltration and clinically by a spectrum of arrhythmias, sudden cardiac death and RV failure. Diagnosis of ARVD still remains a clinical challenge.

METHODS   A three-dimensional electroanatomic mapping technique was used to map the RV of two groups of patients: 1) those with ARVD presenting with typical clinical, electrocardiographic and echocardiographic or magnetic resonance imaging (MRI) findings; and 2) those with structurally normal ventricles.

RESULTS   The dysfunctional RV area could be identified only in the first group and was characterized by the presence of discrete areas of abnormally low-amplitude electrograms. Hence, the normal voltage values observed in the control group (unipolar: 11.9 ± 0.3 mV; bipolar: 4.6 ± 0.2 mV [mean $\pm$ SEM]) and in the nonaffected zones in the ARVD group (unipolar: 10.4 ± 0.2 mV; bipolar: 4.6 ± 0.2 mV) were reduced significantly ($p < 0.05$) in the dysplastic areas (unipolar: 3.3 ± 0.1 mV; bipolar: 0.5 ± 0.1 mV). The pathologic process mainly involved the RV anterolateral free wall, apex and inflow and outflow tracts and ranged from patchy areas to uniform and extensive involvement. Concordance between electroanatomic findings and MRI or echocardiographic findings was noted in all patients.

CONCLUSIONS   The pathologic substrate in ARVD can be identified by spatial association of low-amplitude endocardial electrograms, reflecting replaced myocardial tissue. The ability to accurately identify the presence, location and extent of the pathologic substrate may have important diagnostic, prognostic and therapeutic implications.   (J Am Coll Cardiol 2001;38:2020–7) © 2001 by the American College of Cardiology

The right ventricle (RV) has recently been found to be a focus of a variety of arrhythmias (1–6). Specifically, RV cardiomyopathy or arrhythmogenic right ventricular dysplasia (ARVD) has been identified as a relatively frequent cause of ventricular dysrhythmias and sudden cardiac death in young people (2–6).

Arrhythmogenic right ventricular dysplasia is a heart muscle disease that is often familial; it is characterized by structural and functional abnormalities of the RV due to fibrofatty replacement of myocardial tissue. The characteristic clinical findings include a variety of RV arrhythmias, global or regional RV dysfunction and electrocardiographic (ECG) evidence of depolarization or repolarization abnormalities. Standardized diagnostic criteria have been proposed for the diagnosis of ARVD. These criteria encompass structural, histologic, ECG, arrhythmic and genetic factors (6). Despite these criteria, the diagnosis of ARVD remains a clinical challenge, specifically at its early stage, or in the "formes frustes" (5).

In the current study, we suggest a possible new approach for identification of the pathologic process of ARVD by testing the hypotheses that the abnormal RV substrate can be identified by the presence of low-amplitude local electrograms and that three-dimensional spatial association of these electrograms can be used to define its location and extent.

METHODS

Patient group. All patients gave written, informed consent to the electrophysiologic study. Seven patients (5 men and 2 women; age 33 ± 5 years [range 21 to 49]) with ARVD were studied. Arrhythmogenic right ventricular dysplasia was diagnosed in all patients according to the criteria proposed by the international study group on ARVD (6). Two of the patients were brothers, who had a third brother who died at the age of 20 years from sudden cardiac death. All patients who were included in the study were shown to have some form of RV structural abnormality by using two-dimensional echocardiography (n = 7) or magnetic resonance imaging (MRI; n = 2). The clinical characteristics of the study group are summarized in Table 1.

Six subjects (3 men and 3 women; age 47.0 ± 7.1 years [range 18 to 63]) undergoing electrophysiologic study and radiofrequency ablation for different supraventricular arrhythmias served as the control group. None of the patients had a history of ventricular arrhythmias, and all had normal ventricular function.

> **Abbreviations and Acronyms**
> ARVD = arrhythmogenic right ventricular dysplasia
> LV   = left ventricle or ventricular
> MRI = magnetic resonance imaging
> RV   = right ventricle or ventricular

Mapping technique. The three-dimensional nonfluoroscopic electroanatomic mapping technique (Carto, Biosense-Webster) has already been described elsewhere (7–9). In brief, the method uses ultra-low magnetic fields to accurately determine the location and orientation of a miniature, passive location sensor located at the tip of a 7F electrophysiologic catheter. By sampling the location of the catheter together with the local electrograms recorded from its tip at a plurality of endocardial sites, the three-dimensional geometry of the chamber could be reconstructed in real-time with the electrophysiologic information color-coded and superimposed on the reconstruction (electroanatomic map).

Mapping procedure. The locatable catheter was introduced into the RV using fluoroscopic guidance, and the initial points were sampled to provide the outlayers of the RV (e.g., apex and inflow and outflow tracts). The rest of the mapping procedure was performed with minimal use of fluoroscopy (<5 min), until a complete electroanatomic map of the RV was generated. Based on previous reports (7–10), adequate catheter–tissue contact was ensured by eliminating points in which: 1) the values of the local stability variables were greater than predetermined values (end-diastolic location stability >3 mm and local activation time stability >3 ms); and 2) extreme pressure was applied, as identified by significant ST segment elevation on the unipolar recording.

The unipolar (filtered at 0.5 to 400 Hz) and bipolar (filtered at 30 to 400 Hz) intracardiac electrograms were sampled at each endocardial site. This information was used to generate a three-dimensional voltage map depicting the peak-to-peak amplitude of the unipolar and bipolar electrograms recorded at each site. The reproducibility of the voltage measurements was assessed in a preliminary study in which the catheter was renavigated to the same site five times, and the voltage values obtained were compared. By repeating this procedure in 12 points in two patients, we noted that the voltages measured were highly reproducible, with a minimal standard deviation of 0.57 and 0.90 mV for the unipolar and bipolar recordings, respectively.

Post-procedural analysis of the electrograms recorded was performed in a blinded manner and included measurement of the electrogram's duration, defined as the earliest electrical activity to the onset of the decay artifact (11) at each site, by the use of electronic calipers. Data were compiled on the following electrographic characteristics: amplitude, duration and amplitude/duration ratio. To compare the regional dispersion of voltage values in both groups, the RV was divided into five areas: anterolateral, septal, apical, inferior and outflow. The average voltage value at each area was derived from all points sampled at this zone in all patients.

Statistical analysis. Data are expressed as the mean value ± SEM. One-way analysis of variance (ANOVA) was used to assess for possible differences in the electrophysiologic properties (electrogram's amplitude, duration and amplitude/duration ratio) in the dysplastic region and non-affected zones in the same hearts of patients and control subjects. If found to be statistically significant, post-hoc analysis was performed by using Tukey's multiple comparisons procedure. Similarly, one-way ANOVA and Tukey's multiple comparisons procedure were used to assess for possible differences in the electrophysiologic properties in the different RV regions in control subjects. A value of $p < 0.05$ was considered to be significant.

RESULTS

Electroanatomic findings in the control group. Electroanatomic mapping was performed in six control subjects. The maps acquired were of high density, consisting of 90 ± 16 points and averaging 25 ± 7 min. Figure 1 depicts a typical RV unipolar voltage map of one control subject. Colors represent the peak-to-peak amplitude of the unipolar voltage. Note the presence of relatively high voltage values (blue and purple indicate >8 mV) throughout the RV. A similar finding was noted in all control subjects, with

Table 1. Clinical Characteristics of the Arrhythmogenic Right Ventricular Dysplasia Group

Patient No.	Age (years)	Gender	Family History	Arrhythmia	RV Dilation	Regional Dysfunction	Regional Low Voltage
1	28	F	−	SVT-LBBB, inferior axis	−	Anterolateral: small area	Anterolateral, RVOT
2	48	M	−	SVT-LBBB, inferior axis	+++	Large area: anterolateral, apex	Anterolateral, apex, inflow tract, RVOT
3	30	M	+	SVT-LBBB, left axis	+	Apex, septum	Apex, septum: patchy
4	22	M	+	VPBs, NSVT-LBBB, normal axis	−	Anterolateral, RVOT	Anterolateral-superior, RVOT
5	21	M	−	VPBs, NSVT-LBBB, left axis	+	Anterolateral, RVOT	Anterolateral, RVOT: diffuse
6	49	M	−	VPBs, NSVT-LBBB, normal axis	+	Anterolateral, inflow tract	Anterolateral, inflow tract: patchy
7	47	F	−	SVT-LBBB, normal axis	+	Anterolateral, RVOT, inflow tract	Anterolateral, RVOT, inflow tract

NSVT = nonsustained ventricular tachycardia; RVOT = right ventricular outflow tract; SVT-LBBB = sustained ventricular tachycardia of left bundle branch morphology; VPBs = ventricular premature beats; + = mild dilation; ++ = moderate dilation; +++ = severe dilation.
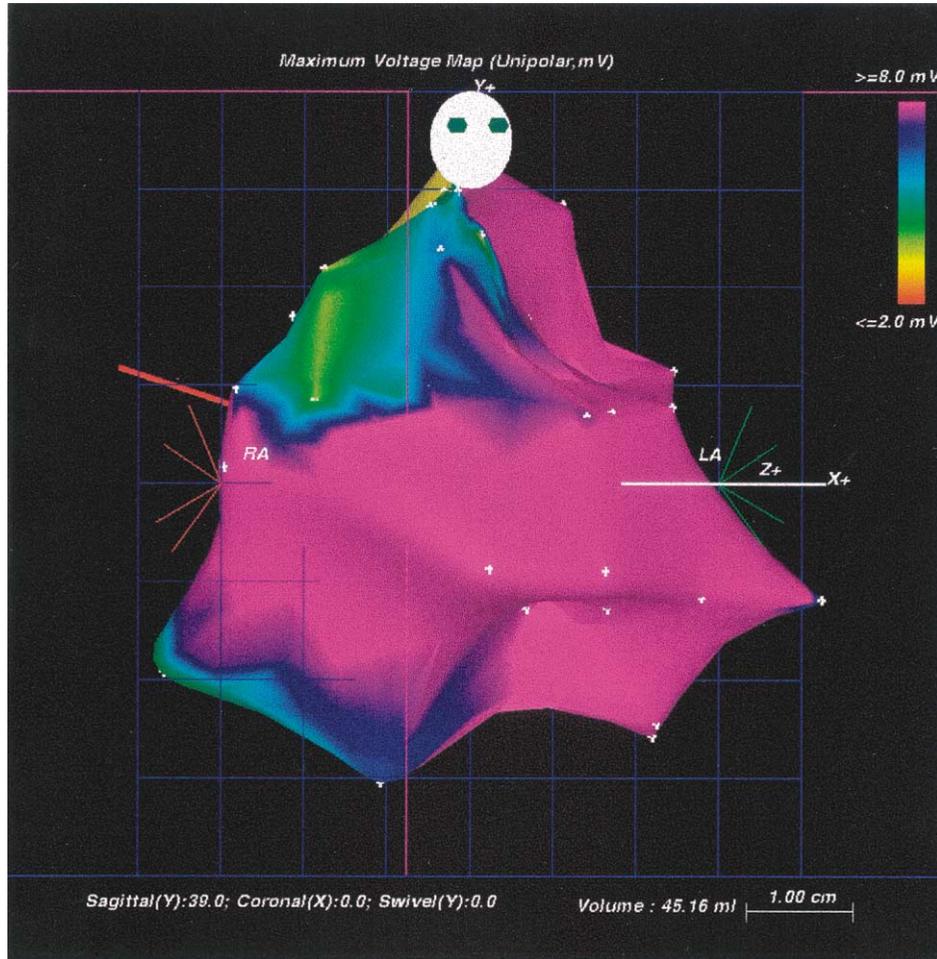
Figure 1. A representative RV electroanatomic voltage map from one of the control subjects; the right anterior oblique projection is shown. The colors represent the amplitude of the local unipolar electrogram. Note the normal unipolar voltage values **(blue and purple)** throughout the RV. LA = left atrium; RA = right atrium.

both the unipolar and bipolar electrograms displaying preserved voltage values in all RV zones (Table 2). The distribution of the voltage values within each zone was relatively homogeneous, with an average standard deviation of 1.9 and 1.8 mV for the unipolar and bipolar recordings, respectively. Interestingly, however, between the zones, spatial dispersion was noted (Table 2), with the septum characterized by the highest voltage values (unipolar: 15.5 ± 0.6 mV; bipolar: 5.8 ± 0.4 mV; $p < 0.05$ vs. anterolateral and inferior regions and outflow tract), and the outflow tract with the lowest values (unipolar: 8.1 ± 0.3 mV; bipolar: 3.3 ± 0.4 mV; $p < 0.05$ vs. all other regions). Electrograms

Table 2. Regional Distribution of Electrogram's Amplitude, Duration and Amplitude/Duration Ratio Values in the Control Group

Electrographic Variables	Anterolateral Region	Apex	Septum	Outflow Tract	Inferior Region
Unipolar: amplitude (mV)	11.4 ± 0.3	13.8 ± 0.5	15.5 ± 0.6	8.1 ± 0.3	12.6 ± 0.5
(significant regional differences with)	(2, 3, 4)	(1, 4)	(1, 4, 5)	(1, 2, 3, 5)	(3, 4)
Unipolar: duration (ms)	51.2 ± 1.5	47.9 ± 1.3	46.5 ± 1.5	54.1 ± 1.2	48.6 ± 1.5
(significant regional differences with)	(4)	(4)	(4)	(2, 3, 5)	(4)
Unipolar: amplitude/duration ratio	0.271 ± 0.027	0.299 ± 0.015	0.378 ± 0.027	0.160 ± 0.010	0.286 ± 0.019
(significant regional differences with)	(3, 4)	(4)	(1, 4, 5)	(1, 2, 3, 5)	(3, 4)
Bipolar: amplitude (mV)	3.9 ± 0.3	4.9 ± 0.5	5.8 ± 0.4	3.3 ± 0.4	4.0 ± 0.4
(significant regional differences with)	(3)	(4)	(1, 4, 5)	(2, 3)	(3)
Bipolar: duration (ms)	39.8 ± 1.2	38.3 ± 1.5	36.7 ± 1.3	43.9 ± 1.6	39.6 ± 1.3
(significant regional differences with)	(4)	(4)	(4)	(1, 2, 3, 5)	(4)
Bipolar: amplitude/duration ratio	0.117 ± 0.011	0.135 ± 0.015	0.206 ± 0.039	0.108 ± 0.014	0.122 ± 0.012
(significant regional differences with)	(3)	(3)	(1, 4, 5)	(3)	(3)

Data are presented as the mean value $\pm$ SEM. Significant regional difference with: $p < 0.05$.

Table 3. Differences in Electrographic Characteristics in the Dysplastic Versus Normal Right Ventricular Regions

Electrographic Variables	Dysplastic Region in ARVD Group	Nonaffected Areas in ARVD Group	Control Group
Unipolar: amplitude (mV)	3.3 ± 0.1*†	10.4 ± 0.2‡	11.9 ± 0.3
Unipolar: duration (ms)	76.6 ± 1.4*†	50.1 ± 0.8	50.1 ± 0.7
Unipolar: amplitude/duration ratio	0.047 ± 0.002*†	0.234 ± 0.009‡	0.271 ± 0.011
Bipolar: amplitude (mV)	0.5 ± 0.1*†	4.6 ± 0.2	4.6 ± 0.2
Bipolar: duration (ms)	74.1 ± 1.9*†	34.3 ± 0.6‡	38.9 ± 0.5
Bipolar: amplitude/duration ratio	0.008 ± 0.001*†	0.158 ± 0.008‡	0.130 ± 0.006

*$p < 0.001$ compared with nonaffected areas in the same hearts (ARVD group). †$p < 0.001$ compared with the control group.
‡$p < 0.05$ compared with the control group. Data are presented at the mean value ± SEM.
ARVD = arrhythmogenic right ventricular dysplasia.

recorded from the outflow tract also displayed some regional variation with the electrograms from the septal area, which displayed higher amplitudes (unipolar: 8.9 ± 0.5 mV; bipolar: 4.2 ± 0.6 mV) than those from the free wall (unipolar: 7.8 ± 0.6 mV; bipolar: 2.9 ± 0.6 mV; $p < 0.05$).

The electrograms recorded from the control subjects were relatively sharp, usually consisting of a single deflection. The electrogram's average unipolar amplitude was 11.9 ± 0.3 mV (Table 3), with 95% of all electrograms recorded having an amplitude >7.0 mV. The mean bipolar amplitude was 4.6 ± 0.2 mV, with 95% of all electrograms having an amplitude >1.2 mV. The fifth percentile values were then used to identify abnormal areas in the ARVD group. The electrogram's mean unipolar duration was 50.1 ± 0.7 ms (range 46.5 ± 1.5 [septum] to 54.1 ± 1.2 [outflow tract]), and the average ratio of unipolar amplitude/duration was 0.271 ± 0.011. The electrogram's mean bipolar duration was 38.9 ± 0.5 ms (range 36.7 ± 1.3 [septum] to 43.9 ± 1.6 [outflow tract]), and the mean bipolar amplitude/duration ratio was 0.130 ± 0.006 (Tables 2 and 3).

Clinical presentations in the ARVD group. The clinical findings in the ARVD group are summarized in Table 1. Of the seven patients with ARVD, four had episodes of sustained ventricular tachycardia of left bundle branch morphology, whereas the other three only had frequent premature beats or short runs of nonsustained tachycardia. Although only one of the patients had symptoms of RV failure, all seven had some type of RV structural abnormalities on the echocardiogram or MRI. Of the seven patients studied, one had marked dilation of the RV, whereas four others had relatively mild dilation of the ventricle, and two others had no dilation noted. Figure 2A displays the echocardiographic findings in the patient with the most extensive pathologic findings (Patient 2). Note the marked dilation of the RV and right atrium, with bulging of the apex and RV free wall. Interestingly, this patient's septum displayed normal contractile function.

Electroanatomic findings in the ARVD group. The mean number of points acquired in the RV electroanatomic maps in the ARVD group was 110 ± 27, taking an average mapping period of 28 ± 3 min. The dysfunctional RV area was identified in all patients with ARVD by spatial association of the abnormally low-amplitude intracardiac electro-

grams. Figure 2B presents the anteroposterior and left anterior oblique views of the RV voltage map of Patient 2. Note the diffused area of markedly reduced voltage values (red indicates unipolar voltage <2 mV) in the anterolateral free wall of the RV. This patient's septum was spared from this process, as indicated by the presence of normal voltage (purple indicates >5 mV). Note that the borders of the pathologic substrate could be localized rather sharply by the large spatial gradient of voltage values.

The dysfunctional RV area could be identified only in the ARVD group and was characterized by significantly lower unipolar and bipolar amplitudes (3.3 ± 0.1 and 0.5 ± 0.1 mV, respectively; $p < 0.001$), compared with the average voltage values in the nonaffected zones in the same patients (10.4 ± 0.2 and 4.6 ± 0.2 mV, respectively) and with the mean RV values in the control subjects (11.9 ± 0.3 and 4.6 ± 0.2 mV, respectively) (Table 3).

Interestingly, the electrograms recorded within the dysplastic areas were also characterized by longer unipolar and bipolar durations. Figure 3 (left panel) depicts the unipolar voltage map in one of the patients with ARVD, whereas Figure 3 (middle panel) and Figure 3 (right panel) represent the three-dimensional dispersion of the unipolar electrogram's duration and amplitude/duration ratio values. Note that the dysplastic zone could be defined by the presence of a low-amplitude electrogram (red indicates <3 mV), as well as by prolonged durations of the electrogram (red indicates >85 ms) and low amplitude/duration ratios (red indicates <0.05).

Significant differences observed in all electrographic characteristics in the dysplastic areas were noted in all patients. The dysplastic zones displayed significantly ($p < 0.001$) longer durations of the electrogram (unipolar: 76.6 ± 1.4 ms; bipolar: 74.1 ± 1.9 ms), compared with the nonaffected zones in the same hearts of patients (unipolar: 50.1 ± 0.8 ms; bipolar: 34.3 ± 0.6 ms) and with the average values in control subjects (unipolar: 50.1 ± 0.7 ms; bipolar: 38.9 ± 0.5 ms) (Table 3). Consequentially, the electrogram's amplitude/duration variable was associated with the largest decrease in the dysplastic region (unipolar: 0.047 ± 0.002; bipolar: 0.008 ± 0.001; $p < 0.001$), compared with the nondiseased areas in the same hearts of patients (unipolar: 0.234 ± 0.009; bipolar: 0.158 ± 0.008) and control
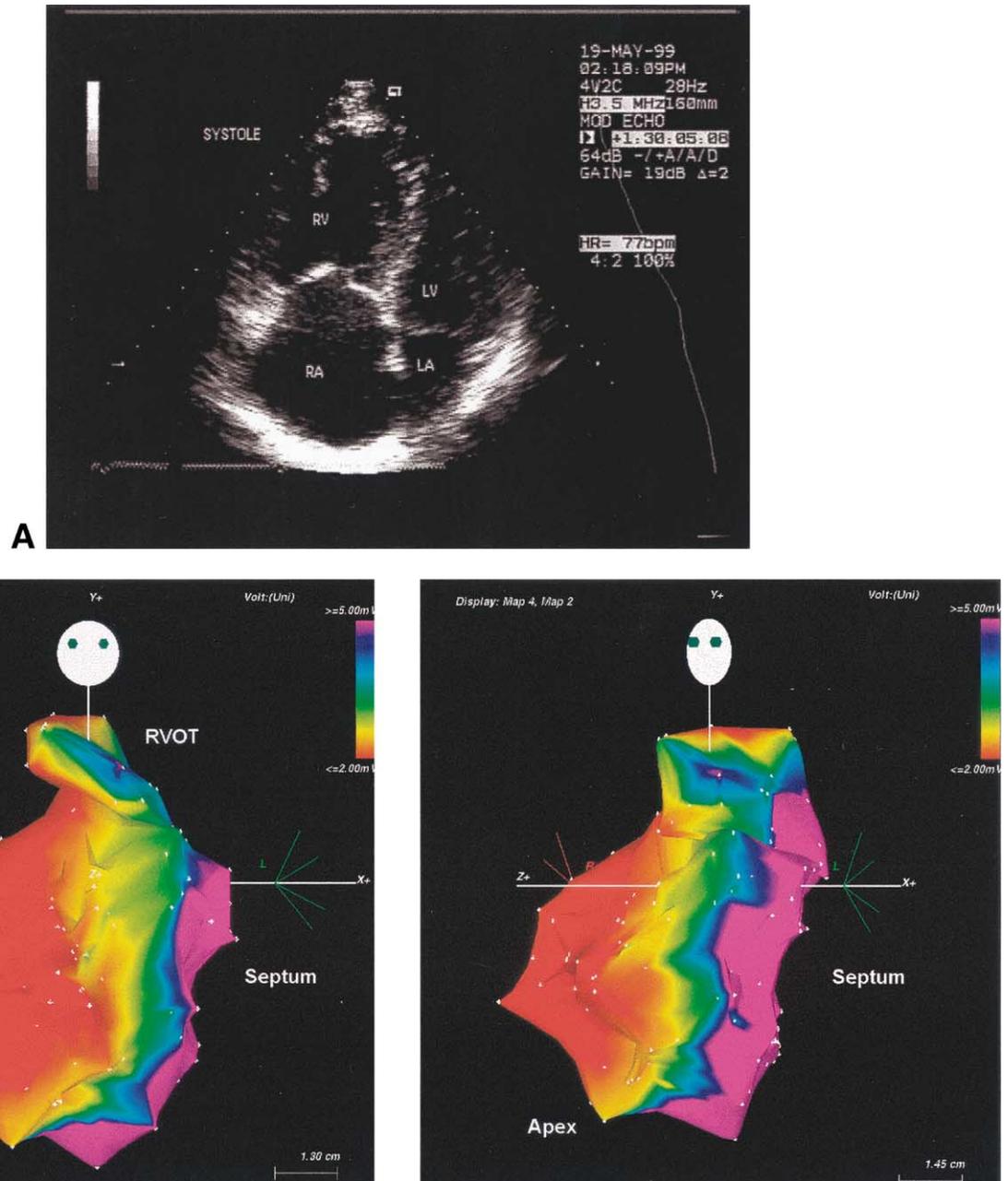
Figure 2. Echocardiographic and electroanatomic mapping of the RV in one of the patients with ARVD. **(A)** Two-dimensional echocardiographic apical view of Patient 2. Note the severe enlargement of the RV and atrium. **(B)** Anteroposterior **(left)** and left anterior oblique **(right)** views of the RV unipolar voltage maps of the same patient. Note the extensive area of low voltage (red indicates <2 mV) in the apex and anterolateral free wall, with the septum being spared (purple indicates >5 mV). LA = left atrium; RA = right atrium; RVOT = right ventricular outflow tract.

subjects (unipolar: 0.271 ± 0.011; bipolar: 0.130 ± 0.006) (Table 3).

Marked differences in the electrophysiologic properties in the dysplastic region were also noted when the electrograms recorded in these areas were divided according to the region in which they were acquired and compared with the same areas in control subjects. Hence, the unipolar electrographic properties of amplitude, duration and amplitude/duration ratio in the dysplastic regions of the anterolateral wall (3.4 ± 0.2 mV, 75.5 ± 1.7 ms and 0.049 ± 0.003, respectively), apex (3.3 ± 0.2 mV, 71.9 ± 3.0 ms and

0.048 ± 0.005) and outflow tract (2.9 ± 0.3 mV, 87.8 ± 3.7 ms and 0.036 ± 0.004) were significantly different (p < 0.01) from those observed in the corresponding regions in the control subjects.

Concordance between electroanatomic mapping and echocardiographic or MRI findings was noted in all patients (Table 1). The pathologic process mainly involved the anterolateral free wall (ranging from relatively limited disease, concentrating only in the superior [n = 3] or apical [n = 2] portions of the free wall, to more uniform, diffuse and extensive disease [n = 2]). The apex was affected in two
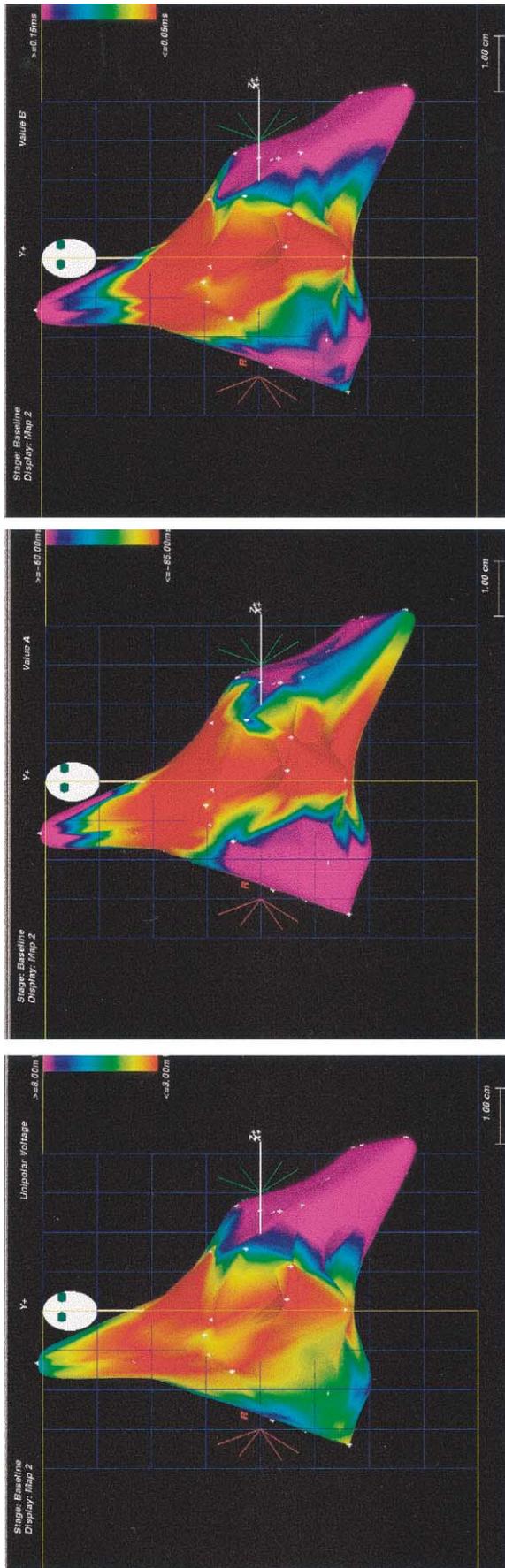
Figure 3. Another example of a patient in the ARVD group. The electroanatomic maps, shown from the right anterior oblique view, depict the three-dimensional spatial dispersion of the unipolar electrogram's amplitude (**left panel**), duration (**middle panel**) and amplitude/duration ratio (**right panel**). Note that the dysplastic region (**red area** in the maps) can be identified by the electrogram's abnormally low amplitude (red indicates <3 mV), prolonged duration (red indicates >85 ms) and low amplitude/duration ratio (red indicates <0.05).

patients; the outflow in three patients; and the inflow tract in three patients. Interestingly, the septum was relatively spared in all but one patient.

DISCUSSION

The diagnosis of ARVD is usually based on typical clinical findings, coupled with the presence of gross structural abnormalities, which can be identified by histologic examination (12) or echocardiography (13), contrast right ventriculography (14) and MRI (15,16). In the present study, we proposed a possible new concept for the diagnosis of ARVD by demonstrating that the pathologic substrate could be identified by the presence of low-amplitude endocardial electrograms. Moreover, by spatially associating these electrograms, we were able to determine the presence, location and extent of the dysplastic regions.

Electrographic characteristics in the healthy and dysplastic RV. Although all zones of the RV in the control subjects demonstrated a significantly higher voltage than that of the dysplastic regions, a reproducible spatial distribution of voltage values in the healthy ventricles could also be noted. Thus, the septum was associated with the highest voltage; the outflow tract with the lowest values (with the free wall area of the outflow tract displaying a lower voltage than that of the septal area); and the rest of the RV with intermediate values. Interestingly, the voltage observed in the RV was significantly lower than that observed previously in the healthy left ventricle (LV) (17,18). These results may be explained by the spatial distribution of myocardial tissue mass, with the septum of the LV and RV being significantly thicker than all other RV regions, or alternatively, by the heterogeneous distribution of fatty tissue in the normal RV.

The results of the present study clearly indicate that the dysplastic areas can be identified by the presence of abnormally low-amplitude electrograms. Hence, significantly lower voltage values were noted in the RV dysplastic regions, compared with all other RV zones in the same patients and with all RV regions in control subjects. Interestingly, a relatively sharp border, as identified by a steep spatial voltage gradient, could be used to demarcate the dysplastic regions. Furthermore, concordance between the presence, location and extent of the dysplastic region, as identified by the voltage maps and the echocardiographic or MRI findings, was noted in all patients.

The electrograms recorded from dysplastic areas were also associated with significantly longer potential durations, compared with those from healthy regions. The combination of electrograms that were characterized by a low amplitude and long duration resulted in very low amplitude/duration ratio values. Consequentially, this variable was associated with maximal reductions of 80% and 95%, from healthy RV values, for the unipolar and bipolar recordings, respectively.

Although both unipolar and bipolar electrograms displayed similar changes in the dysplastic regions, some

differences could be observed. It is well accepted in the literature that bipolar recordings are more reflective of local electrical activity because unfiltered unipolar recordings are more influenced by far-field potentials (19). This effect was demonstrated by the larger changes observed in all electrographic variables in the bipolar versus unipolar recordings and by the slightly lower (but statistically significant) unipolar voltage values observed in the nonaffected areas of the ARVD group versus the control group. However, bipolar recordings may also possess certain limitations, due to greater directional sensitivity. This may result in significant changes in the electrographic morphology during changes in electrode orientation relative to the activation wave front. Consequentially, this may tend to increase the number of false-positive points (low bipolar amplitude in normal zones) and may also result in more heterogeneity within each zone.

The observation that significant loss of myocytes results in the recording of low-amplitude, fractionated endocardial electrograms with a prolonged potential duration is not new and is well established in scarred tissue in the LV (11,20,21). Thus, a similar finding in dysplastic regions can be explained by the replacement of action potential–generating myocardial tissue with the characteristic fibrofatty infiltration. Another observation known from studies of scar tissue is the significant increase in pacing threshold values in this area. Although not studied in the present report, this may be used as another criterion to distinguish between healthy and dysplastic regions.

The ability of the electroanatomic mapping technique to accurately associate these electrograms with their spatial orientation in the heart allowed the accurate anatomic identification and quantification of dysfunctional zones. A typical spatial distribution of the dysplastic regions was noted in the group of patients studied, with the anterolateral free wall, apex and outflow tract regions being predominantly affected; the septum was relatively spared in all but one patient. This observed spatial distribution of dysplastic changes was also noted in previous studies, with the LV and ventricular septum being involved to a lesser extent than the rest of the RV (2,4,12).

Clinical significance. Although ARVD is a rare disease, it is a relatively frequent cause of sudden cardiac death in young individuals. Despite recent advances in the available diagnostic modalities and the criteria proposed for diagnosis of the disease, identification of ARVD still remains a clinical challenge, especially in those patients in whom the disease is at its early stage, or in the "formes frustes" (5). In these patients, the minor structural abnormalities may be missed by echocardiography or ventriculography.

Endomyocardial biopsy has the potential for the in vivo demonstration of the characteristic fibrofatty infiltration (12). However, for reasons of safety, samples are usually taken from the interventricular septum, a region not commonly involved in the disease, thus limiting the sensitivity of the test. Magnetic resonance imaging has been suggested as a more sensitive method to identify the pathologic abnormalities in patients with RV tachyarrhythmias (15,16). The presence of focal or diffuse fatty infiltrates and abnormal thickening of regions of focal dyskinesia have been proposed as criteria for the diagnosis of RV dysplasia by MRI. However, the diagnostic sensitivity and specificity of MRI still need to be defined, and, at present, the quality of images obtained may be operator-dependent.

The results of the present study suggest that electroanatomic mapping may be added to the existing diagnostic modalities in patients with ARVD. Hence, the ability to identify the dysplastic process by the presence of low-amplitude electrograms may be used as a new criterion in these patients' work-up. Specifically, this may be of practical help in differentiating ARVD from RV outflow tract tachycardia, which is usually a benign arrhythmic condition with a different pathologic mechanism and treatment (22,23). Nevertheless, further studies will need to test the hypothesis of whether the RV abnormalities identified in this study are absent in patients with RV outflow tract tachycardia.

Although electrographic recordings with a low amplitude and longer duration in dysplastic regions do not require the use of three-dimensional electromagnetic mapping techniques, the ability to spatially associate these electrograms and to generate a three-dimensional electroanatomic map of the chamber may be of clinical importance, for a number of reasons. First, this ability may be helpful in determining that the entire chamber has been mapped and that isolated dysplastic areas have not been missed. Second, the ability to identify not only the presence, but also the location and extent of the dysplastic process may provide important prognostic information on the extent of the disease and may also aid in guiding possible therapeutic procedures, such as pacemaker or defibrillation lead placement, endomyocardial biopsy and future curative ablation procedures. Recent studies have demonstrated that electroanatomic mapping of the LV can be used to ablate ischemic ventricular tachycardias. Specifically, a linear lesion extending from the infarct-related areas in the LV during sinus rhythm was recently used to control unmappable ventricular tachycardias (24). One could thus envision, in the future, a similar strategy being applied to the RV.

Study limitations. This study involved patients with only confirmed ARVD; therefore, the sensitivity and specificity of the technique could not be assessed. Hence, patients with a milder form of the disease, with minimal pathologic involvement that could not be identified by echocardiography or MRI, were not included in this study. In addition, it has been reported that in some patients with ARVD, pathologic examination may be limited to epicardial and midmural lesions, sparing the endocardial layers (5). Although not noted in the current study, this may potentially lead to less reduction in the voltage values. Similarly, the specificity of the technique was not evaluated in patients with other RV myopathies. It is likely that similar results would be found in other diseases that cause scarring in the

RV, such as sarcoidosis. Nevertheless, despite these limitations, this study demonstrated that electroanatomic mapping is useful in the evaluation of patients with suspected ARVD.

Conclusions. From this study, in which electroanatomic mapping was performed in the RV of patients with ARVD, we can conclude that the dysplastic regions can be identified, quantified and differentiated from healthy myocardium by the presence of a low amplitude and longer duration on the electrogram, reflecting replaced myocardial tissue. The results of the present study also suggest that this technique may supplement or replace existing diagnostic tests in patients with suspected ARVD. Nevertheless, further studies will need to determine the clinical diagnostic utility and possible therapeutic applications of this technique in patients with ARVD.

Reprint requests and correspondence: Dr. Lior Gepstein, Cardiovascular Research Laboratory, The Bruce Rappaport Faculty of Medicine, Technion-Israel Institute of Technology, 2 Efron Street, P.O. Box 9649, 31096 Haifa, Israel. E-mail: mdlior@tx.technion.ac.il.

REFERENCES

1. Fontaine G, Fontaliran F, Frank R. Arrhythmogenic right ventricular cardiomyopathies: clinical forms and main differential diagnosis (editorial). Circulation 1998;97:1532–5.
2. Marcus FI, Fontaine G, Guiraudon G, et al. Right ventricular dysplasia: a report of 24 adult cases. Circulation 1982;65:384–98.
3. Thiene G, Nava A, Corrado D, Rossi L, Pennelli N. Right ventricular cardiomyopathy and sudden death in young people. N Engl J Med 1988;318:129–33.
4. Corrado D, Basso C, Thiene G, et al. Spectrum of clinicopathologic manifestation of arrhythmogenic right ventricular cardiomyopathy/dysplasia: a multicenter study. J Am Coll Cardiol 1997;30:1512–20.
5. Fontaine G, Fontaliran F, Hebert JL, et al. Arrhythmogenic right ventricular dysplasia. Annu Rev Med 1999;50:17–35.
6. McKenna WJ, Thiene G, Nava A, et al., Task Force of the Working Group on Myocardial and Pericardial Disease of the European Society of Cardiology and of the Scientific Council on Cardiomyopathies of the International Society and Federation of Cardiology. Diagnosis of arrhythmogenic right ventricular dysplasia/cardiomyopathy. Br Heart J 1994;71:215–8.
7. Gepstein L, Hayam G, Ben-Haim SA. A novel method for nonfluoroscopic catheter-based electroanatomical mapping of the heart: in vitro and in vivo accuracy results. Circulation 1997;95:1611–22.
8. Gepstein L, Evans SJ. Electroanatomical mapping of the heart: basic concepts and implications for the treatment of cardiac arrhythmias. Pacing Clin Electrophysiol 1998;21:1268–78.
9. Ben-Haim SA, Osadchy D, Schuster I, et al. Nonfluoroscopic, in vivo navigation and mapping technology. Nat Med 1996;2:1393–5.
10. Lessick J, Kornowski R, Fuchs S, Ben-Haim SA. Assessment of NOGA catheter stability during the entire cardiac cycle by means of a special needle-tipped catheter. Cathet Cardiovasc Interv 2001;52:400–6.
11. Cassidy DM, Vassallo JA, Marchlinski FE, Buxton AE, Unterecker WJ, Josephson ME. Endocardial activation in humans in sinus rhythm with normal left ventricles: activation patterns and characteristics of electrograms. Circulation 1984;70:37–42.
12. Angelini A, Basso C, Nava A, Thiene G. Endomyocardial biopsy in arrhythmogenic right ventricular cardiomyopathy. Am Heart J 1996;132:203–6.
13. Blomstrom-Lundqvist C, Beckman-Suurkula M, Wallentin I, Jonsson R, Olsson SB. Ventricular dimensions and wall motion assessed by echocardiography in patients with arrhythmogenic right ventricular dysplasia. Eur Heart J 1988;9:1291–302.
14. Daliento L, Rizzoli G, Thiene G, et al. Diagnostic accuracy of right ventriculography in arrhythmogenic right ventricular cardiomyopathy. Am J Cardiol 1990;66:741–5.
15. Ricci C, Longo R, Pagnan L, et al. Magnetic resonance imaging in right ventricular dysplasia. Am J Cardiol 1992;70:1589–95.
16. Blake LM, Scheinman MM, Higgins CB. MR features of arrhythmogenic right ventricular dysplasia. Am J Radiol 1994;162:809–12.
17. Gepstein L, Goldin A, Lessick J, et al. Electromechanical characterization of chronic myocardial infarction in the canine coronary occlusion model. Circulation 1998;98:2055–64.
18. Kornowski R, Hong MK, Gepstein L, et al. Preliminary animal and clinical experiences using an electromechanical endocardial mapping procedure to distinguish infarcted from healthy myocardium. Circulation 1998;98:1116–24.
19. Wit AL, Janse MJ. The Ventricular Arrhythmias of Ischemia and Infarction: Electrophysiological Mechanisms. Mount Kisco, NY: Futura Publishing, 1993, 225–31.
20. Cassidy DM, Vassallo JA, Miller JM, et al. Endocardial catheter mapping in patients in sinus rhythm: relationship to underlying heart disease and ventricular arrhythmias. Circulation 1986;73:645–52.
21. Callans DJ, Ren JF, Michele J, Marchlinski FE, Dillon SM. Electroanatomic left ventricular mapping in the porcine model of healed anterior myocardial infarction: correlation with intracardiac echocardiography and pathological analysis. Circulation 1999;100:1744–50.
22. Brooks R, Burgess JH. Idiopathic ventricular tachycardia: a review. Medicine (Baltimore) 1988;67:271–94.
23. Lemery R, Brugada P, Bella PD, et al. Nonischemic ventricular tachycardia: clinical course and long-term follow-up in patients without clinically overt heart disease. Circulation 1989;79:990–9.
24. Marchlinski FE, Callans DJ, Gottlieb CD, Zado E. Linear ablation lesions for control of unmappable ventricular tachycardia in patients with ischemic and nonischemic cardiomyopathy. Circulation 2000;101:1288–96.